Novel Silica Surface Charge Density Mediated Control of the Optical Properties of Embedded Optically Active Materials and Its Application for Fiber Optic pH Sensing at Elevated Temperatures

Electronic Supplementary Information

Congjun Wang,[ab] Paul R. Ohodnicki, Jr.,[ac] Xin Su,[a] Murphy Keller,[a] Thomas D. Brown[a] and John P. Baltrus[a]*

[a]National Energy Technology Laboratory, U.S. Department of Energy, 626 Cochrans Mill Road, Pittsburgh, PA 15236, United States. [b]URS Corporation, P.O. Box 618, South Park, PA 15129, United States. [c] Carnegie Mellon University, Department of Materials Science and Engineering, 5000 Forbes Avenue, Pittsburgh, PA 15213, United States.

1. Schematic of the pH sensing experimental setup

Figure S1. Schematic of the pH sensing experimental setup.

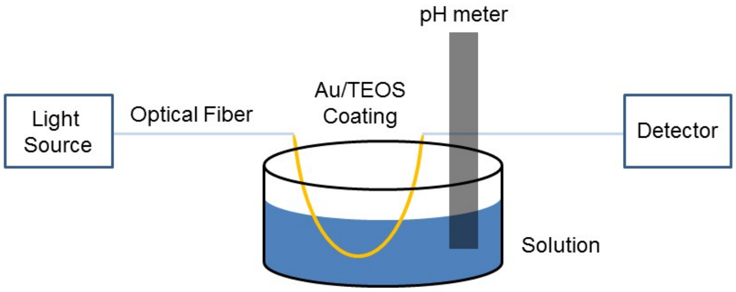

2. SEM image of the Au nanoparticles/TEOS coated optical fiber

Figure S2. SEM images of an optical fiber coated with Au/TEOS calcined at 200 °C. The Au nanoparticles are the small white dots in the image. Scale bars, 50 μm (left) and 1 μm (right).

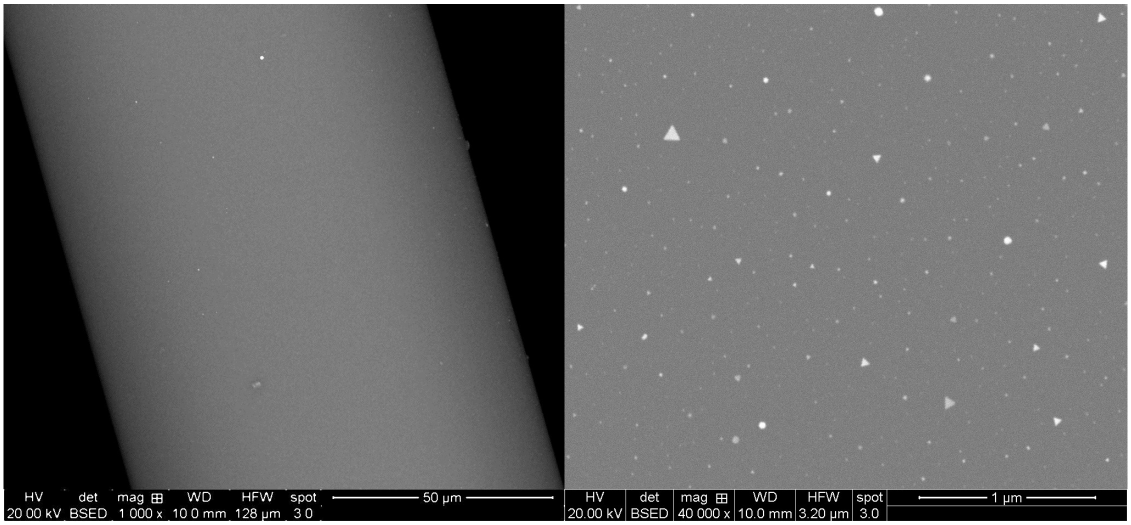

3. pH sensing with fibers calcined at 600 °C

Figure S3. Transmission spectra of a Au/TEOS coated optical fiber during calcination at 600 °C

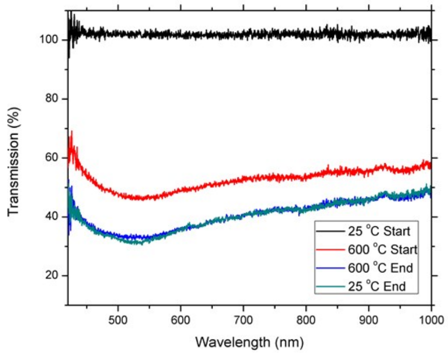

.

Figure S4. C 1s XPS spectra of two Au-TEOS samples calcined at two temperatures, 600 °C (top spectrum) and 200 °C (bottom spectrum). The spectra have been curve fitted with peaks representing C-C (284.7 eV), C-O (286.5 eV) and C(=O)-O (288.8 eV). Note the overall decrease in signal to noise for the sample calcined at 600 °C due to the loss of carbon plus relative decreases in the higher binding energy carbon peaks due to C-O and carboxyl (likely a result of contamination from air exposure). The surface atomic ratio of C/Au decreased from 7.69 to 4.50 for the 200 °C and 600 °C calcined samples, respectively. The accumulation of surface adventitious carbon from exposure to air will be reflected to a greater extent in the sample calcined at 600 °C further suggesting the more complete loss of organic species and therefore the formation of an inorganic matrix for the sample calcined at 600 °C.

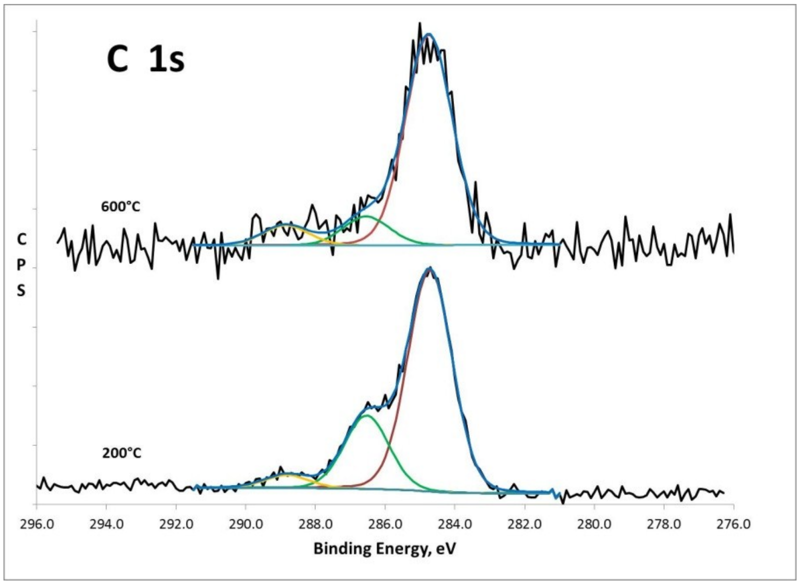

Figure S5. (a) The transmission spectra of a Au/TEOS optical fiber calcined at 600 °C at different pH values; (b) The transmission monitored at the LSPR peak 525 nm of the same optical fiber as a function of time as pH is varied. The solution pH is indicated in the figure.

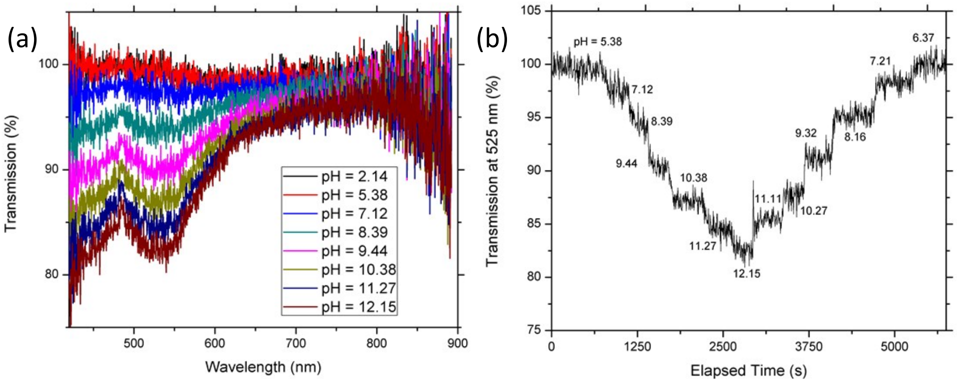

4. Rhodamine B as the optically active material

Figure S6. The absorption spectra of rhodamine B molecule in different pH solutions, showing a small red-shift as pH decreases for pH < ~6.

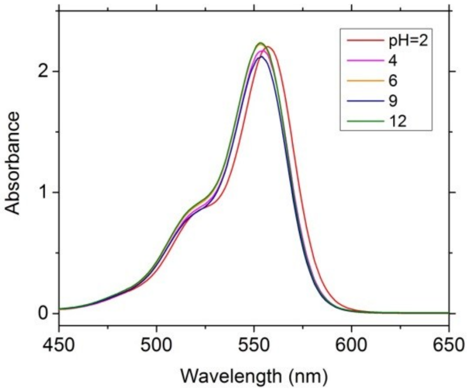

Figure S7. The relative transmission at 586 nm for a rhodamine B/TEOS coated optical fiber as a function of experimental time as pH is repeatedly changed at room temperature. The pH of the solution is denoted by the numbers in the figure.

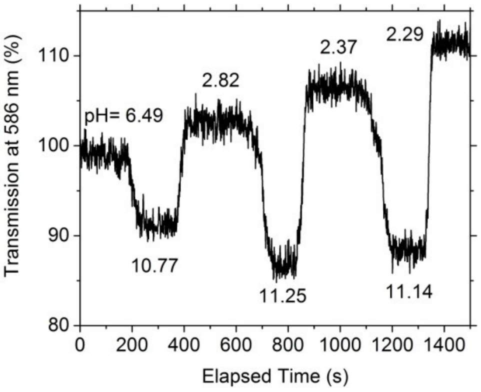

5. Robust optical response to pH with Pd/TEOS coated fibers

Figure S8. Transmission at various wavelengths in the visible region of a Pd/TEOS coated fiber calcined at 200 °C as a function of time when the pH of the solution is repeatedly changed at room temperature. The pH of the solution is denoted by the numbers in the figure.

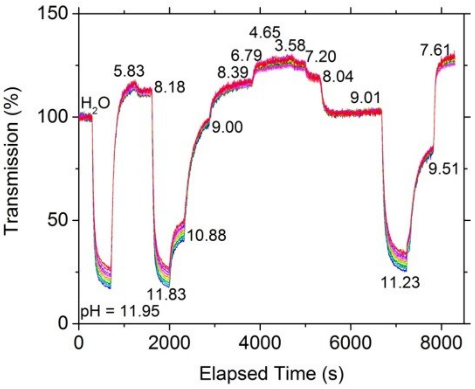

6. Control experiments

Figure S9. (a) Transmission spectra of an optical fiber coated with pure TEOS and calcined at 200 °C at pH 2.87 (red) and 11.21 (blue). (b) Transmission at various wavelengths in the visible region as a function of time when the pH of the solution is repeatedly changed. The pH of the solution is denoted by the numbers in the figure and the dashed lines indicate the time when the pH is varied.

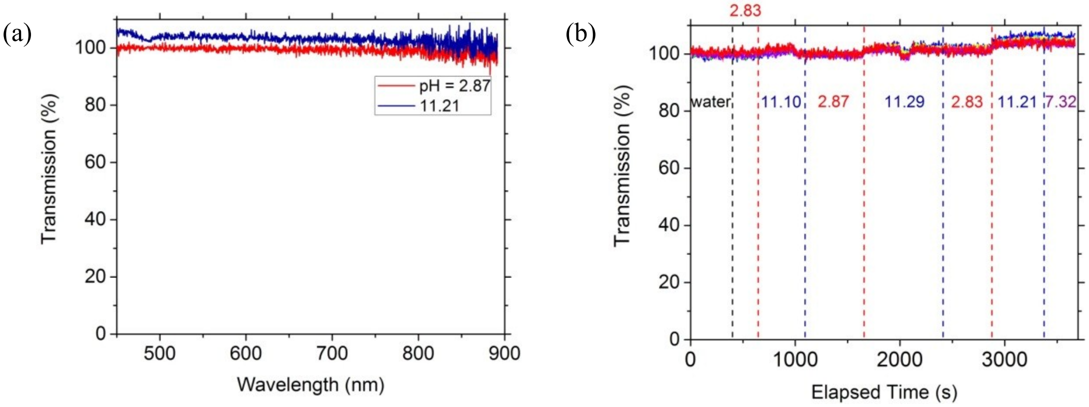

Figure S10. pH sensing using a Au nanoparticles coated optical fiber calcined at 200 **°C** using KOH and H_2SO_4 acid/base pair. The transmission at the plasmon absorption peak 550 nm as a function of time when the pH of the solution is repeated adjusted by adding KOH/H_2SO_4. The pH of the solution is denoted by the numbers in the figure.

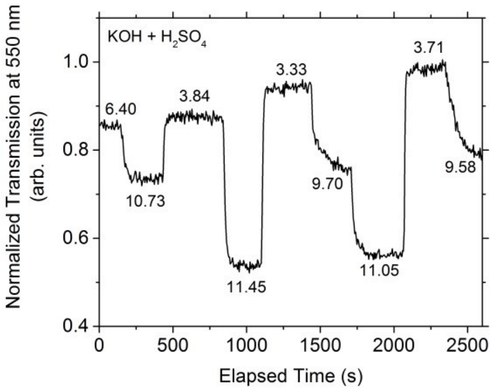

Figure S11. Transmission at the peak plasmon absorption wavelength 550 nm of a Au nanoparticles coated optical fiber calcined at 200 °C as a function of time with variations of pH and the refractive index *n*. The pH is adjusted by the addition of NaOH and H_3PO_4, whereas the *n* is intentionally increased by adding NaCl to the solution. The purple dotted line and the purple dashed line indicate the start of the addition of NaCl and the saturation of NaCl (23.95 %), respectively. The purple arrows indicate the repeated addition of NaCl to the solution. Each addition ranges from 0.5 g to 10 g of NaCl. After the solution is saturated, additional NaOH and H_3PO_4 are added to further change the solution pH. The pH of the solution is denoted by the black numbers in the figure. The approximate refractive index *n* before the addition of NaCl is ~1.33 and increases to > 1.37 at NaCl saturation.

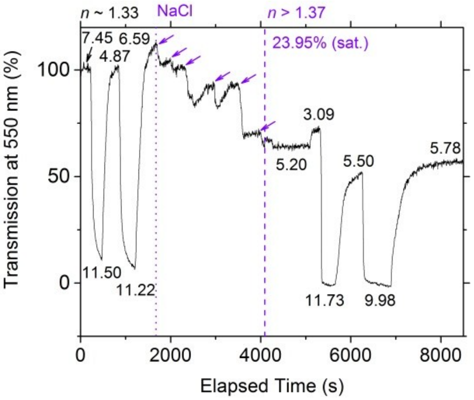

Figure S12. Transmission spectra of a Au coated optical fiber calcined at 200 **°C** in solution as different amounts of NaCl are added as indicated by the wt.% in the legend. A red-shift in the plasmon absorption band is clearly observed as the *n* increases, as expected, despite the fact that the change in transmission (~35%) is much smaller compared to the change in response to pH (~80%).

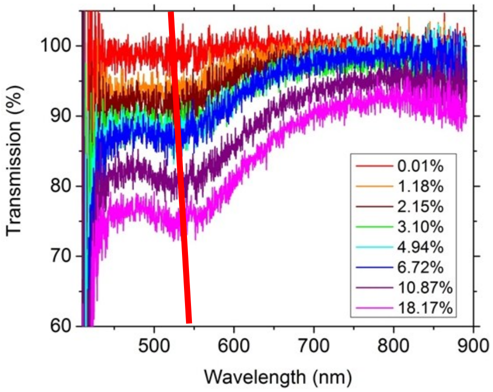

Figures S11 and S12 provide additional evidence that the solution refractive index change does not apply in the observed optical response as pH is changed. First, the amount of the added acid/base is relatively small and the change in n_s is expected to be minimal (< 0.1 % change) under our experimental conditions. This is particularly evident at the beginning of each experiment when only a miniscule amount of acid or base is added to the water to induce significant changes in pH with a negligible change in n_s and yet the corresponding optical change is dramatic. For example, the first change of pH from neutral to 11.50 as shown in Figure 4 in the main text requires the addition of ~ 0.06 ml of 0.1 M NaOH to 100 ml of water. The concentration of the NaOH would then be 6×10^{-6} M and based on the available data on the change of n_s as a function of NaOH concentration, this would result in an essentially negligible change of the solution n_s by ~10^{-5}%. The change of n_s would be minimal even at the highest concentrations of the acid/base used in our experiments. At the end of each experiment, the typical concentration of the total NaOH/H_3PO_4 and the resulting salts (Na_3PO_4, Na_2HPO_4 and NaH_2PO_4) in the solution is approximately 0.03 M which translates to a maximum change of n_s from 1.333 to only ~1.3343 (~0.1% change in n_s). In contrast, as large amounts of NaCl are introduced, n_s is substantially increased to > 1.3721 at saturation (~3 % change) resulting in expected shifts in the plasmon resonance absorption peak to longer wavelengths and an associated reduction in transmission. However, the addition of small amounts of acid and base with negligible change in n_s leads to larger changes in transmission near the plasmon absorption peak wavelength than that induced by saturating the solution with NaCl resulting in more than an order of magnitude larger increase in n_s. For example, the first addition of NaOH (6×10^{-6} M) results in > 80 % decrease in transmission at the plasmon absorption band peak wavelength of $\lambda = 550$ nm, whereas at NaCl saturation ($n \sim 1.3721$), the change is only ~35 % for the same sensor (Figure 4 in the main text). Second, the repeated addition of H_3PO_4 and NaOH can only result in continued increase of n_s which indicates that any optical changes purely due to the variation of n_s would also be monotonic, inconsistent with the experimental results that the optical changes are large and reversible depending on the pH (Figure 4 in the main text and Figure S11). In comparison, the repeated addition of NaCl causes a monotonic decrease in transmission upon each addition (note that some spectral drift is occurring between NaCl additions in Figure S11 due to the fact that it takes time for the solid NaCl to completely dissolve and achieve a uniform refractive index throughout the solution). Third, even at NaCl saturation, further adjusting the solution pH by the addition of small amounts of H_3PO_4 and NaOH again results in strong, and reversible optical responses (Figure S11). This not only demonstrates that the response is not a result of change in n_s but also illustrates the capability of these sensors to operate in high salinity solutions. Finally, the pH sensing response does not show any measurable spectral shift which is different from the observed, and expected, red-shift of ~ 15 nm of the plasmon resonance peak associated with the relatively large increase in n_s for saturated NaCl solutions (Figure S12).

7. Understanding the pH response mechanism

Figure S13. Normalized change in transmission as a function of solution pH (red triangles and left *y* axis) at the peak plasmon absorption band wavelengths of 550 for the Au coated fibers calcined at 200 °C in saturated NaCl solution at. The blue solid curve (right *y* axis) is the calculated surface charge density of silica as a function of pH based on the Stern model at 80 °C, with a total site density $\Gamma_0 = 8\ \mathrm{nm}^{-2}$, a Stern capacitance $C_S = 2.9\ \mathrm{F/m^2}$, an ionization constant $\mathrm{p}K = 7.5$ and an ionic strength $I = 7$ M. The dashed curve (right *y* axis) is the calculated surface charge density at 25 °C with an ionic strength $I = 5 \times 10^{-2}$ M as used in Figure 3d in the main text.

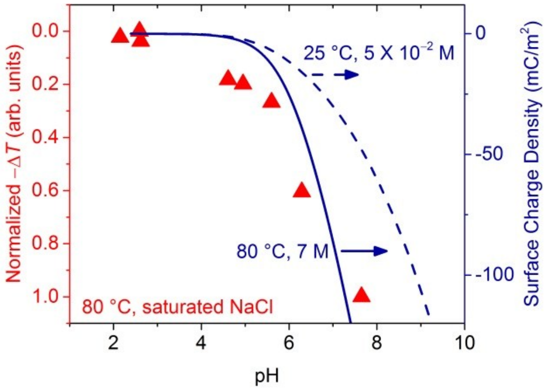

Figure S14. Transmission spectra of a Au/OTCS coated optical fiber during calcination at 200 °C.

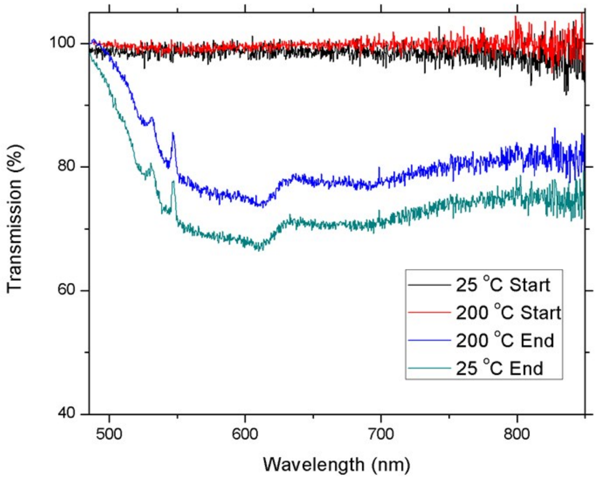

Figure S15. SEM images of an optical fiber coated with Au/OTCS calcined at 200 °C. The Au nanoparticles are the small white dots in the image. Scale bars, 50 (left) and 1 μm (right).

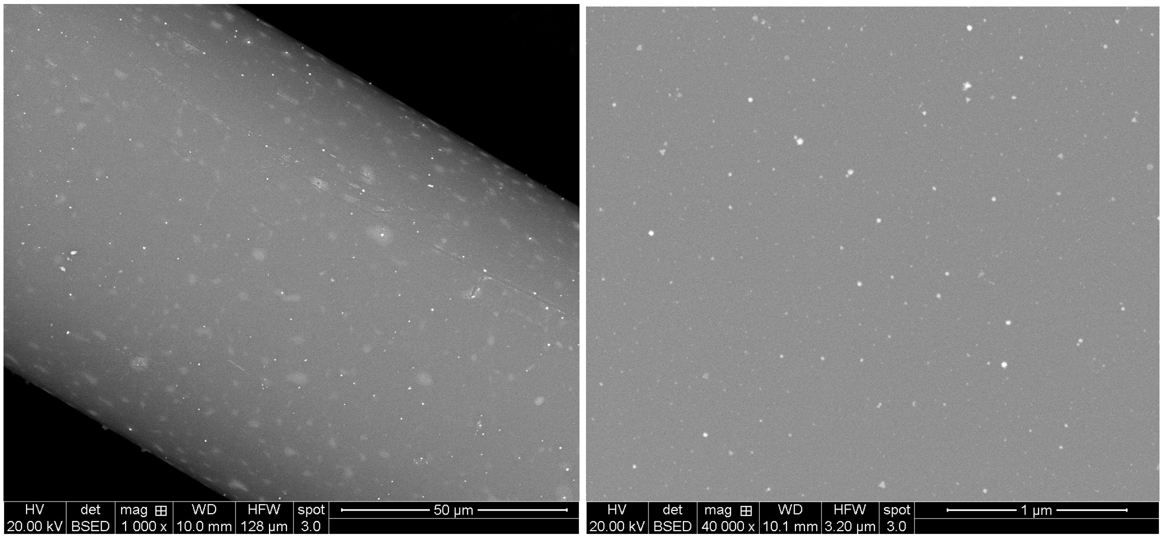

Figure S16. (a) Transmission spectra of an Au/OTCS coated optical fiber calcined at 200 **°C** at different pH values. (b) Transmission at the plasmon absorption peak of 550 nm as a function of time when the pH is changed. The pH is denoted by the numbers in the figure and the dashed lines indicate the time when the pH is adjusted.

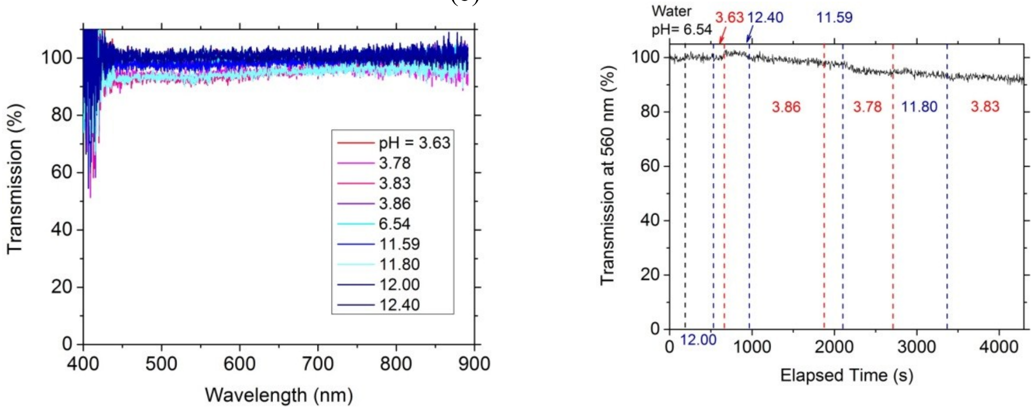
(a) (b)